Journal of Food and Drug Analysis

Volume 28 | Issue 2 Article 6

Chemometric Authentication of Pu'er Teas in Terms of Multielement Stable Isotope Ratios Analysis by EA-IRMS and ICP-MS

Recommended Citation
Liu, Honglin; Zeng, Yitao; Zhao, Xin; and Tong, Huarong (2020) "Chemometric Authentication of Pu'er Teas in Terms of Multielement Stable Isotope Ratios Analysis by EA-IRMS and ICP-MS," *Journal of Food and Drug Analysis*: Vol. 28 : Iss. 2 , Article 6.
Available at: https://doi.org/10.38212/2224-6614.1059

ORIGINAL ARTICLE

Chemometric authentication of Pu'er teas in terms of multielement stable isotope ratios analysis by EA-IRMS and ICP-MS

Honglin Liu [a,b], Yitao Zeng [c], Xin Zhao [b], Huarong Tong [a,*]

[a] College of Food Science, Southwest University, Chongqing 400715, China
[b] Chongqing University of Education, Chongqing Collaborative Innovation Center for Functional Food, Chongqing Engineering Research Center of Functional Food, Chongqing Engineering Laboratory for Research and Development of Functional Food, Chongqing 400067, China
[c] Chongqing Furen High School, Chongqing 400067, China

Abstract

In this work, the stable isotope ratios of carbon, nitrogen, hydrogen, oxygen, and mineral elements and their stoichiometric methods were examined as possible factors that could certify Chinese tea based on its production years. A total of 43 multi-element stable isotope ratios of Xiangzhujing Pu'er tea in five production years were determined through inductively coupled plasma mass spectrometry (ICP-MS) and elemental analyzer-isotope ratio mass spectrometry (EA-IRMS) methods. Two unsupervised learning techniques (principal component analysis and hierarchical clustering analysis) and three supervised learning techniques (partial least squares discriminant analysis [PLS-DA], back-propagation artificial neural network [BP-ANN], and linear discriminant analysis [LDA]) were used on the basis of 18 statistically significant multi-elemental stable isotope ratios to build authentication models for Pu'er tea. The clustering abilities of the two unsupervised learning methods were worse than those of the three supervised learning methods. The three supervised models correctly separated the corresponding production years of the samples. The authentication performance was obtained through BP-ANN and LDA, with 100% recognition and prediction abilities, which were better than those of PLS-DA. δD, $\delta^{13}C$, and $^{154}Sm/^{152}Sm$ were determined as the markers for the accurate authentication of Pu'er tea in different production years. The profiles of multi-element stable isotope ratios obtained via ICP-MS and EA-IRMS with chemometric methods could serve as potential and powerful factors for authenticating Chinese tea in different production years. This study contributed to the generalization of the use of multi-elemental stable isotope ratio fingerprinting as a promising tool for testing the authenticity of tea worldwide.

Keywords: Authentication, EA-IRMS and ICP-MS, Multielement stable isotope ratio, Pu'er tea, Stoichiometric methods

1. Introduction

With consumers' growing interest in health, the demand for information about food authenticity, origin, growth methods, and processing techniques has also increased. For instance, the authentication of tea has been a great deal of interest. Tea is one of the three most popular nonalcoholic beverages worldwide, and it has many health benefits [1,2]. Teas can be aged to ensure the original quality and even improve the quality of tea based on basic tea packaging. For example, the aging of dark tea improves its quality. Properly stored tea does not deteriorate. After aging, the aroma of teas is more fragrant, and their taste is more mellow. Chinese dark tea (CDT) is a post-fermented tea and one of the six major teas in China. Pu'er tea is the most common

Received 6 January 2020; accepted 11 March 2020.
Available online 27 June 2020

* *Corresponding author at:* College of Food Science, Southwest University, Chongqing 400715, China. Fax: +86 6825 0679.
E-mail address: huart@swu.edu.cn (H.R. Tong).

https://doi.org/10.38212/2224-6614.1059

CDTs that have been accepted and valued by an increasing number of consumers with a healthy lifestyle [3,4]. Given the different production years of Pu'er tea, tea quality within a certain period of time enhances with aging time under appropriate storage conditions [5−8]. Therefore, within a certain period, the older the Pu'er tea, the more expensive the price. Consumers are interested in the production time of Pu'er tea. The production year of teas should be authenticated with different analytical methods.

Most studies on the authentication of tea leaves in different production years have focused on the determination of chemical compositions (e.g., caffeine, catechins, and aroma components) and the examination of morphological characteristics (e.g., shape, size, and color) [9−15]. However, determination and examination methods often lack reproducibility mainly because of variable analytical capabilities, annual changes in the chemical composition of targets, and different environmental or culture conditions of samples [16,17].

In comparison with organic compounds, multiple elements have stable isotope ratios that can also reflect the different growth conditions of plants. Elements are superior to these compounds because they are less affected by processing and storage time, and their contents are stable [18]. Therefore, to accurately authenticate teas in different production years, we proposed an analytical method based on element analyzer-isotope ratio mass spectrometry (EA-IRMS) and inductively coupled plasma mass spectrometry (ICP-MS). In the proposed method, multi-element stable isotope ratios (mainly C, N, H, O, and $^{87}Sr/^{86}Sr$) combined with stoichiometric models were used to accurately trace the origin of various teas [18−26]. In general, given the natural differences in physical, chemical, or microbial isotope fractionation processes, the measurement of the stable isotope ratios of C, N, H, and O was considered a promising tool for authenticating various agricultural, such as tea. For example, plant metabolic processes, such as C3, C4, and crassulacean acid metabolism photosynthesis, lead to differences in $\delta^{13}C$. Variations can also occur because of environmental factors, such as water availability, drought stress, nutrient availability, and anthropogenic effects. In plants, the effect of metabolic activity impact on $\delta^{13}C$ is greater than that of environmental factors [27,28]. The stable N isotope composition of plants is mainly influenced by soil environment and local nitrogen fertilizer systems, such as type, brand, chemical form, strength, and application timing of different fertilizers [29−32]. Metabolic differences in agricultural can result in different δD and $\delta^{18}O$ in sap or plant tissues, and δD and $\delta^{18}O$ of such are closely related to climatic conditions, including precipitation, irrigation/surface water sources, height, and distance to the coast [29]. The stable isotope ratios of small mineral elements, such as Sr, are among the most reliable and widely used isotope fingerprints for the determination of tea, food or animal sources [18,33]. However, no study has used stable isotope ratios to authenticate teas in different production years.

Herein, we reported our preliminary investigation on the changes in the 43 multi-elemental stable isotope ratios of C, N, H, O, and various mineral elements in Pu'er tea in different production years (from 2014 to 2018) through EA-IRMS and ICP-MS for the first time. On the basis of multi-elemental stable isotope ratios, we conducted multivariate analyses and applied two unsupervised learning techniques (i.e., principal component analysis [PCA] and hierarchical clustering analysis [HCA]) and three supervised learning techniques (i.e., partial least squares discriminant analysis [PLS-DA], back-propagation artificial neural network [BP-ANN], and linear discriminant analysis [LDA]) to authenticate teas in different production years. We also selected the most important multi-elemental stable isotope ratios as markers and simultaneously compared the authentication performance of the models. We expected that the preliminary results would demonstrate the feasibility of our authentication technology for teas in different production years in China to prevent the false labeling of teas and provide a basis for applying the proposed method for other tea samples worldwide.

2. Materials and methods

2.1. Tea samples

A same brand of Pu'er tea from Xiangzhujing and produced by the same manufacturer in Yunnan Province (Fengqing, Lincang, Yunnan; latitude, 24° 35′; longitude, 100° 04′) in China in the harvesting seasons in 2014, 2015, 2016, 2017, and 2018 ($n = 9$ for each year) were collected in 2019. These Pu'er tea product samples were stored for 1−5 years. The grades of samples are PINGCHA, and the tea tree variety are all Fengqing large leaf species. Their authenticity, traceability, and equivalent production regimes were ensured by the Yunnan Academy of Agricultural Sciences. The collected tea samples were stored in a freezer at −40 °C until multi-elemental stable isotope ratio analysis.

2.2. Sample preparation

Approximately 0.2 g of freeze-dried Pu'er tea samples ground with a ball mill (MM301, Retsch, Germany) and screened with a 100-mesh sieve was accurately weighed (accuracy of 0.0001 g) and then placed in a Teflon digestion vessel. The Teflon digestion vessel was soaked in 20% HNO_3 overnight, cleaned with ultrapure water until no sour taste existed, and dried before use. The samples were then treated with a mixture of 5 mL of HNO_3 (65% w/w, Merck) and 2 mL of H_2O_2 (30% w/w, Merck). Heat digestion was conducted in a microwave digestion apparatus (MARS 6 CEM, Matthews, USA) in accordance with the set microwave digestion procedure which digested for 90 min by increasing the power to 1400 W and the temperature to 180 °C in a three stepwise fashion. The apparatus was cooled to room temperature to remove the samples after digestion. Subsequently, the lid of the tank in the fume hood was slowly opened to exhaust the gas, and the digestion tank was placed on an acid extraction heater (BHW, Botong, China) at 140 °C for acid extraction. Afterward, the digestion tank and the lid were washed with a small amount of ultrapure water 3–4 times, and the washing liquid was combined in a Teflon digestion volumetric bottle at a fixed volume of 50 mL for standby application. The above steps were performed for mineral element stable isotope ratio analysis. The samples were ground to powder, passed through a 100-mesh sieve, and dried in an oven at 65 °C for another 48 h for C,N,H,O stable isotope ratio analyses.

2.3. Mineral element stable isotope ratio analysis through ICP-MS

Thirty-nine mineral element stable isotope ratios ($^{109}Ag/^{107}Ag$, $^{138}Ba/^{137}Ba$, $^{81}Br/^{79}Br$, $^{112}Cd/^{111}Cd$, $^{114}Cd/^{112}Cd$, $^{114}Cd/^{111}Cd$, $^{53}Cr/^{52}Cr$, $^{72}Ge/^{70}Ge$, $^{74}Ge/^{72}Ge$, $^{74}Ge/^{70}Ge$, $^{202}Hg/^{200}Hg$, $^{7}Li/^{6}Li$, $^{96}Mo/^{95}Mo$, $^{98}Mo/^{96}Mo$, $^{98}Mo/^{95}Mo$, $^{60}Ni/^{58}Ni$, $^{207}Pb/^{206}Pb$, $^{208}Pb/^{207}Pb$, $^{208}Pb/^{206}Pb$, $^{123}Sb/^{121}Sb$, $^{80}Se/^{78}Se$, $^{120}Sn/^{118}Sn$, $^{88}Sr/^{86}Sr$, $^{47}Ti/^{46}Ti$, $^{48}Ti/^{47}Ti$, $^{48}Ti/^{46}Ti$, $^{205}Tl/^{203}Tl$, $^{66}Zn/^{64}Zn$, $^{68}Zn/^{66}Zn$, $^{68}Zn/^{64}Zn$, $^{153}Eu/^{151}Eu$, $^{154}Sm/^{152}Sm$, $^{158}Gd/^{156}Gd$, $^{160}Gd/^{158}Gd$, $^{160}Gd/^{156}Gd$, $^{164}Dy/^{162}Dy$, $^{168}Er/^{166}Er$, $^{174}Yb/^{172}Yb$, $^{176}Lu/^{175}Lu$) analysis of the prepared extracts was performed in a ratio mode by using an ICP-MS instrument (Perkin-Elmer NexION 300X, USA). The internal standards (Re, In, and Rh) and the tuning solution (Be, Ce, Fe, In, Li, Mg, Pb, and U) were used to correct the matrix effects and compensate for the possible variations in instrument performance during determination.

2.4. C,N,H,O stable isotope ratio analysis via EA-IRMS

Approximately 4.5 mg ($\delta^{13}C$ and $\delta^{15}N$) of Pu'er tea was packed into a 4 mm × 11 mm tin powder capsule, and 1.5 mg (δD and $\delta^{18}O$, balanced for 3 days in the dryer) of Pu'er tea was packed into a 3.5 mm × 5.0 mm silver powder capsule for C,N,H,O stable isotope ratio analysis. Automatic injection was conducted using a flash 2000 element analyzer (EA, ThermoFisher, USA). The teas were loaded into a dynamic fast burning furnace (Prepacke reactor, ThermoFisher, UK), and isotope ratio mass spectrometry (Delta V Advantage, ThermoFisher, USA) was introduced. The high-temperature combustion furnace $\delta^{13}C$ and $\delta^{15}N$ isotopes of the elemental analyzer were set at 980 °C, with a carrier gas flow (He) of 230 mL/min. Pyrolysis (δD and $\delta^{18}O$) was conducted at a carrier gas flow rate (He) of 120 mL/min at 1450 °C. The isotopic ratio was measured as follows: δsample (‰) = (Rsample/Rstandard − 1) × 1000, where the sample represents $\delta^{13}C$, $\delta^{15}N$, δD, or $\delta^{18}O$, and the R value of the isotope ratio represents $^{13}C/^{12}C$, $^{15}N/^{14}N$, $D/^{1}H$, or $^{18}O/^{16}O$ analytical sample in accortdance with the International Atomic Energy Agency (IAEA, Vienna, Austria) standard. The accuracy determined through reproducibility of the analysis for $\delta^{13}C$, $\delta^{15}N$, δD, and $\delta^{18}O$ were 0.15‰, 0.2‰, 1.5‰, and 0.3‰, respectively. $\delta^{13}C$, $\delta^{15}N$, δD, or $\delta^{18}O$ (‰) have established reference standards in the international community, that is, Vienna Pee Dee Belemnite for C, N_2 (air) for N, and Vienna Standard Mean Ocean Seawater (VSMOW) for H and O.

The main reference materials (IAEA, Vienna, Austria), including IAEA-N1 (NH_4SO_4, $\delta^{15}N = 0.4 \pm 0.2$‰), USGS24 (graphite, $\delta^{13}C = 16 \pm 0.1$‰), VSMOW (ocean water, $\delta^{2}H = 0$‰), SLAP ($\delta^{2}H = -428.0$‰), IAEA601 ($\delta^{18}O$vsmow = 23.3 ± 0.3‰), and IAEA602 ($\delta^{18}O$vsmow = 71.4 ± 0.5‰), were used for the multipoint calibration of isotope ratios.

2.5. Statistical analysis

In this study, the 43 multi-elemental stable isotope ratios for each sample were separately analyzed for each analyte. In addition, triplicate measurements were made if the average standard deviation of the duplicates was outside the expected measurement error (±1‰). For multiple comparisons, Tukey's post hoc test was used, all differences were considered statistically significant if $p < 0.05$ at 95% confidence interval.

One-way ANOVA, LDA, and BP-ANN were applied using SPSS Statistics version 23.0 (IBM,

USA). PCA and PLS-DA were conducted using SIMCA version 13.0 (Umetrics, Umeå, Sweden). Before PCA, LDA, PLS-DA, and BP-ANN were carried out, all variables were "autoscaled." HCA is used to visualize the correlation between variables and samples. PCA is an unsupervised pattern recognition technique that reduces dimensionality and provides the local view and trend of spatial data [34]. Three supervised learning techniques were applied to establish the authenticity prediction model of Pu'er tea. The dataset with statistically significant variables was assessed through PLS-DA, BP-ANN, and LDA to construct the model. PLS-DA is a regression discrimination tool used to predict a set of variables and identify them as function classes from numerous independent variables [35]. As a supervised pattern recognition technique, BP-ANN has been widely used in stoichiometry. This technique usually consists of three layers, namely, input, hidden, and output layers. The input layer is characterized by rows for classification as an input to the layer; in the output layer, each class in the dataset has an output node [36]. LDA tests the affinity of each sample to the previously defined group by minimizing intragroup variance and maximizing intergroup variance [37].

3. Results and discussion

3.1. Variation in $\delta^{13}C$, $\delta^{15}N$, δD, and $\delta^{18}O$

We initially examined the different $\delta^{13}C$, $\delta^{15}N$, δD, and $\delta^{18}O$ profiles over the Pu'er tea in terms of five production years (from 2014 to 2018; Table 1). The distribution and change in $\delta^{13}C$, $\delta^{15}N$, δD, and $\delta^{18}O$ in Pu'er tea in different years are shown in Fig. 1. $\delta^{13}C$, $\delta^{15}N$, δD, and $\delta^{18}O$ significantly differed in most production years ($p < 0.001$). The boxes correspond to the interquartile range containing the middle 50% of data, whereas the whiskers indicate the highest and lowest values at 95% and 5% over the entire data range, respectively. The squares inside the boxes represent the mean values, whereas the lines across each box and the filled circles on the box/whisker charts indicate the median and outlier values, respectively. × symbol represents 99% and 1% of the whole data range, and −indicates maximum and minimum values. VPDB, Vienna Pee Dee Belemnite; VSMOW, Vienna Standard Mean Ocean Water. The distribution patterns of these values showed a normal Gaussian distribution even with a few outlier values.

The carbon isotope ratio $\delta^{13}C$ low variation ranged from −25.88‰ to−24.78‰.~2‰ variation in $\delta^{13}C$ in produce grown in the same area due to slight variations in nutrient and water levels available for plant growth [27]. According to previous studies [18–26], $\delta^{13}C$ of tea from China varied between −24‰ and −28‰, which is similar to the $\delta^{13}C$ (−25.88‰ to −24.78‰) observed for the Pu'er tea in this study. These $\delta^{13}C$ distributions also conform to the known $\delta^{13}C$ range (−30‰ to −22‰) of C3 plants [27]. Xiangzhujing Pu'er tea in 2015 had lest in negative $\delta^{13}C$ mean, and Pu'er tea in 2018 had most in negative $\delta^{13}C$ mean ($p < 0.001$; Fig. 1A and Table 1). The extremely lower $\delta^{13}C$ may be related to the increase in artificial CO_2 emissions in 2018 [38].

$\delta^{15}N$ low variation (~2‰) ranged between 1.27‰ and 3.44‰, with a highest $\delta^{15}N$ mean for Pu'er tea in 2017 and a lowest $\delta^{15}N$ mean for Pu'er tea in 2015 ($p < 0.001$; Fig. 1B and Table 1). In general, $\delta^{15}N$ of organic fertilizers (1‰–37‰, representatively >5‰) is higher than that of synthetic fertilizers (−4‰–4‰) [39]. Therefore, synthetic fertilizers might be applied to tea leaves in this study. Previous studies [18–26] showed that $\delta^{15}N$ of Chinese tea varies between 0‰ and 8‰. These results were similar to our findings; that is, the range of $\delta^{15}N$ was 1.27‰–3.44‰. Nitrate levels in irrigation water, N isotope fractionation in soil, and fertilizer availability also affect $\delta^{15}N$ of various agricultural [32]. Therefore, low $\delta^{15}N$ of Pu'er tea in 2015 predicted the difference in the results of N isotopic fractionation and fertilizer availability, although we did not examine $\delta^{15}N$ of organic fertilizers or soil cultivation. As such, the physical, chemical, and microbial properties of soil were affected rather than the specific use of chemical fertilizers by nitrogen groups.

δD of Pu'er tea ranged from −38.92‰ to −25.18‰. Pu'er tea in 2018 had a characteristic profile of δD and the mean δD of Pu'er tea in 2015 and 2017 was lower than that of other Pu'er teas ($p < 0.001$; Fig. 1C and Table 1). Similarly, Pu'er tea in 2018 had a characteristic profile of $\delta^{18}O$ and the mean $\delta^{18}O$ of Pu'er teas in 2017 was lower than that of other Pu'er teas ($p < 0.001$; Fig. 1D and Table 1). Increased precipitation with heavy water isotopes (i.e., $H_2^{18}O$, $D_2^{16}O$ or $D_2^{18}O$) results in heavier H and O isotopes in precipitation and groundwater [31]. δD and $\delta^{18}O$ in Pu'er tea differed probably because the level was affected by climate in a particular year and topographic features. However, the most important parameter in determining δD and $\delta^{18}O$ in Pu'er tea remains unclear. Further studies should be conducted to clarify the comprehensive effects of topography and climate parameters on the variation in δD and $\delta^{18}O$ of Pu'er tea in different years.

In conclusion, as $\delta^{18}O$ permits to discriminate among the five harvesting years by itself ($p < 0.001$).

Table 1. Stable isotope ratios and the mean comparison results of the one-way ANOVA of Pu'er tea samples in 2014–2018.

Variables	2014 samples (n = 9)			2015 samples (n = 9)			2016 samples (n = 9)			2017 samples (n = 9)			2018 samples (*n* = 9)			F	P-Value
	mean ± SD	min	max	mean ± SD	min	max	mean ± SD	min	max	mean ± SD	min	max	mean	min	max		
$\delta^{13}C$ (‰)	-25.14 ± 0.14^{a}	−25.25	−24.78	-25.06 ± 0.12^{a}	−25.20	−24.85	-25.08 ± 0.15^{a}	−25.32	−24.84	-25.65 ± 0.14^{b}	−25.88	−25.51	-25.69 ± 0.13^{b}	−25.88	−25.48	49.03	0.000
$\delta^{15}N$ (‰)	2.01 ± 0.31^{bc}	1.32	2.40	1.76 ± 0.36^{c}	1.27	2.26	2.33 ± 0.52^{b}	1.32	3.03	3.04 ± 0.34^{a}	2.51	3.44	2.93 ± 0.19^{a}	2.51	3.10	21.69	0.000
δD (‰)	-32.37 ± 0.79^{b}	−33.31	−31.34	-37.76 ± 0.82^{c}	−38.92	−36.57	-31.96 ± 0.66^{b}	−32.91	−31.24	-37.04 ± 1.20^{c}	−38.49	−34.60	-26.80 ± 1.21^{a}	−28.99	−25.18	190.40	0.000
$\delta^{18}O$ (‰)	28.52 ± 0.46^{b}	27.55	29.19	26.32 ± 0.35^{d}	25.79	26.71	27.67 ± 0.41^{c}	27.23	28.47	25.65 ± 0.27^{e}	25.15	26.02	29.13 ± 0.41^{a}	28.29	29.50	127.99	0.000
$^{109}Ag/^{107}Ag$	0.93 ± 0.14	0.76	1.14	0.99 ± 0.06	0.90	1.07	1.02 ± 0.11	0.87	1.22	0.96 ± 0.13	0.79	1.15	0.98 ± 0.09	0.80	1.07	0.85	0.500
$^{138}Ba/^{137}Ba$	1.05 ± 0.02^{ab}	1.03	1.09	1.01 ± 0.07^{b}	0.89	1.07	1.02 ± 0.07^{ab}	0.91	1.08	1.06 ± 0.01^{a}	1.04	1.09	0.91 ± 0.01^{c}	0.89	1.09	14.01	0.000
$^{81}Br/^{79}Br$	0.97 ± 0.20	0.68	1.32	1.02 ± 0.24	0.78	1.41	1.03 ± 0.19	0.59	1.19	0.98 ± 0.14	0.67	1.13	1.02 ± 0.18	0.72	1.23	0.19	0.940
$^{112}Cd/^{111}Cd$	1.00 ± 0.15	0.68	1.23	0.97 ± 0.07	0.86	1.11	0.98 ± 0.13	0.77	1.22	0.97 ± 0.07	0.86	1.08	0.98 ± 0.14	0.74	1.14	0.14	0.965
$^{114}Cd/^{112}Cd$	1.08 ± 0.18	0.99	1.53	1.01 ± 0.08	0.91	1.17	0.99 ± 0.08	0.89	1.15	0.99 ± 0.04	0.89	1.03	0.94 ± 0.09	0.82	1.08	2.30	0.075
$^{114}Cd/^{111}Cd$	1.07 ± 0.10^{a}	0.95	1.27	0.97 ± 0.07^{ab}	0.90	1.08	0.97 ± 0.14^{ab}	0.74	1.19	0.95 ± 0.05^{b}	0.87	1.02	0.92 ± 0.13^{b}	0.76	1.07	2.64	0.048
$^{53}Cr/^{52}Cr$	0.91 ± 0.03^{a}	0.87	0.96	0.84 ± 0.02^{c}	0.82	0.90	0.85 ± 0.04^{c}	0.82	0.95	0.82 ± 0.01^{d}	0.80	0.84	0.88 ± 0.03^{b}	0.83	0.92	15.94	0.000
$^{72}Ge/^{70}Ge$	1.02 ± 0.13^{a}	0.78	1.24	0.85 ± 0.18^{ab}	0.62	1.09	0.80 ± 0.23^{b}	0.60	1.33	0.75 ± 0.14^{b}	0.60	0.99	0.87 ± 0.20^{ab}	0.49	1.09	2.82	0.037
$^{74}Ge/^{72}Ge$	1.55 ± 0.32	0.98	1.99	1.35 ± 0.22	1.06	1.79	1.52 ± 0.22	1.24	1.92	1.49 ± 0.36	1.03	2.15	1.56 ± 0.33	1.09	2.25	0.74	0.572
$^{74}Ge/^{70}Ge$	1.58 ± 0.40^{a}	1.05	2.17	1.13 ± 0.21^{b}	0.82	1.39	$1.20 \pm 0.0.33^{b}$	0.79	1.85	1.12 ± 0.30^{b}	0.70	1.71	1.33 ± 0.31^{ab}	0.71	1.79	3.35	0.019
$^{202}Hg/^{200}Hg$	1.00 ± 0.10	0.85	1.11	1.01 ± 0.12	0.87	1.20	1.01 ± 0.10	0.82	1.17	1.01 ± 0.12	0.89	1.24	0.99 ± 0.12	0.87	1.17	0.04	0.997
$^{7}Li/^{6}Li$	1.04 ± 0.05	0.96	1.12	1.01 ± 0.06	0.90	1.09	1.04 ± 0.06	0.97	1.15	1.05 ± 0.09	0.99	1.23	0.99 ± 0.04	0.93	1.08	1.63	0.186
$^{96}Mo/^{95}Mo$	1.03 ± 0.09^{a}	0.90	1.18	0.96 ± 0.17^{ab}	0.76	1.35	0.90 ± 0.07^{bc}	0.82	1.01	0.74 ± 0.07^{d}	0.66	0.85	0.82 ± 0.06^{cd}	0.74	0.92	11.25	0.000
$^{98}Mo/^{96}Mo$	0.95 ± 0.07^{a}	0.84	1.06	0.76 ± 0.15^{b}	0.57	1.11	0.68 ± 0.09^{bc}	0.48	0.81	0.66 ± 0.10^{c}	0.52	0.84	0.70 ± 0.05^{bc}	0.62	0.76	13.18	0.000
$^{98}Mo/^{95}Mo$	0.98 ± 0.11^{a}	0.82	1.12	0.71 ± 0.08^{b}	0.62	0.84	0.61 ± 0.06^{c}	0.48	0.70	0.49 ± 0.10^{d}	0.38	0.64	0.57 ± 0.04^{c}	0.46	0.61	45.89	0.000
$^{60}Ni/^{58}Ni$	1.03 ± 0.02	1.00	1.05	1.03 ± 0.02	1.00	1.06	1.03 ± 0.02	1.00	1.06	1.02 ± 0.01	1.00	1.04	1.02 ± 0.02	0.99	1.04	1.78	0.151
$^{207}Pb/^{206}Pb$	1.00 ± 0.02	0.97	1.03	1.00 ± 0.02	0.96	1.02	1.03 ± 0.02	0.97	1.05	1.02 ± 0.03	0.97	1.06	1.00 ± 0.02	0.96	1.04	2.59	0.051
$^{208}Pb/^{207}Pb$	1.01 ± 0.03^{a}	0.95	1.03	1.00 ± 0.02^{ab}	0.96	1.03	0.97 ± 0.02^{c}	0.94	1.00	0.98 ± 0.02^{bc}	0.96	1.01	0.98 ± 0.02^{abc}	0.94	1.03	4.57	0.004
$^{208}Pb/^{206}Pb$	1.01 ± 0.02	0.98	1.03	1.00 ± 0.02	0.97	1.04	0.99 ± 0.01	0.97	1.02	1.00 ± 0.03	0.94	1.04	0.99 ± 0.02	0.96	1.01	1.29	0.292
$^{123}Sb/^{121}Sb$	1.00 ± 0.04	0.92	1.05	1.02 ± 0.07	0.94	1.16	0.96 ± 0.05	0.89	1.04	0.97 ± 0.08	0.86	1.12	0.95 ± 0.08	0.87	1.11	1.61	0.190
$^{80}Se/^{78}Se$	1.02 ± 0.04	0.95	1.06	1.02 ± 0.03	0.97	1.06	0.99 ± 0.05	0.93	1.06	0.98 ± 0.03	0.94	1.04	0.99 ± 0.03	0.96	1.05	2.04	0.107
$^{120}Sn/^{118}Sn$	1.02 ± 0.06	0.93	1.10	0.96 ± 0.13	0.76	1.18	0.98 ± 0.09	0.86	1.08	1.01 ± 0.08	0.88	1.11	1.02 ± 0.11	0.86	1.23	0.75	0.566
$^{88}Sr/^{86}Sr$	0.87 ± 0.01	0.85	0.88	0.86 ± 0.01	0.85	0.88	0.86 ± 0.01	0.85	0.89	0.87 ± 0.01	0.86	0.88	0.87 ± 0.01	0.85	0.90	1.87	0.135
$^{47}Ti/^{46}Ti$	0.85 ± 0.10	0.64	0.99	0.95 ± 0.09	0.83	1.08	0.90 ± 0.12	0.76	1.07	1.01 ± 0.17	0.78	1.23	0.96 ± 0.22	0.39	1.08	1.45	0.237
$^{48}Ti/^{47}Ti$	1.08 ± 0.11^{a}	0.86	1.21	1.05 ± 0.06^{a}	0.94	1.13	1.09 ± 0.20^{a}	0.90	1.58	0.91 ± 0.06^{b}	0.82	0.98	0.87 ± 0.06^{b}	0.78	0.94	7.19	0.000
$^{48}Ti/^{46}Ti$	0.91 ± 0.06	0.78	1.00	0.99 ± 0.06	0.89	1.04	0.97 ± 0.13	0.81	1.25	0.91 ± 0.12	0.75	1.08	0.84 ± 0.19	0.35	1.01	2.00	0.114
$^{205}Tl/^{203}Tl$	1.04 ± 0.09	0.93	1.19	1.01 ± 0.12	0.86	1.27	1.07 ± 0.21	0.79	1.47	0.97 ± 0.08	0.86	1.08	0.95 ± 0.11	0.84	1.18	1.29	0.291
$^{66}Zn/^{64}Zn$	1.01 ± 0.02	0.98	1.03	1.01 ± 0.02	0.98	1.03	1.00 ± 0.02	0.97	1.04	1.00 ± 0.02	0.98	1.05	1.00 ± 0.02	0.98	1.03	0.80	0.534
$^{68}Zn/^{66}Zn$	0.99 ± 0.02	0.98	1.03	1.00 ± 0.01	0.99	1.02	1.01 ± 0.02	0.98	1.03	1.00 ± 0.02	0.96	1.01	0.99 ± 0.02	0.96	1.03	1.37	0.262
$^{68}Zn/^{64}Zn$	1.01 ± 0.01	0.98	1.02	1.01 ± 0.01	1.00	1.02	1.00 ± 0.01	0.98	1.02	1.00 ± 0.01	0.98	1.01	0.99 ± 0.01	0.97	1.01	2.48	0.059
$^{153}Eu/^{151}Eu$	1.30 ± 0.06	1.22	1.42	1.27 ± 0.07	1.19	1.40	1.30 ± 0.09	1.22	1.51	1.25 ± 0.06	1.14	1.33	1.23 ± 0.04	1.18	1.31	1.80	0.149
$^{154}Sm/^{152}Sm$	1.07 ± 0.03^{a}	1.02	1.12	0.91 ± 0.03^{b}	0.87	0.95	0.85 ± 0.06^{c}	0.79	0.94	0.93 ± 0.05^{b}	0.87	1.01	0.91 ± 0.04^{b}	0.84	0.99	28.32	0.000
$^{158}Gd/^{156}Gd$	0.60 ± 0.04^{a}	0.54	0.67	0.56 ± 0.04^{ab}	0.51	0.63	0.54 ± 0.04^{b}	0.48	0.60	0.58 ± 0.04^{a}	0.52	0.64	0.60 ± 0.05^{a}	0.55	0.67	3.98	0.008
$^{160}Gd/^{158}Gd$	0.92 ± 0.03	0.88	0.95	0.90 ± 0.03	0.85	0.94	0.88 ± 0.05	0.79	0.95	0.92 ± 0.04	0.87	0.97	0.92 ± 0.04	0.86	0.99	1.82	0.144
$^{160}Gd/^{156}Gd$	0.55 ± 0.05^{a}	0.48	0.61	0.51 ± 0.03^{ab}	0.47	0.55	0.47 ± 0.06^{b}	0.38	0.55	0.53 ± 0.05^{a}	0.46	0.58	0.55 ± 0.03^{a}	0.51	0.63	4.89	0.003
$^{164}Dy/^{162}Dy$	0.94 ± 0.02	0.92	0.97	0.96 ± 0.04	0.88	0.99	0.92 ± 0.04	0.86	0.97	0.94 ± 0.03	0.90	0.97	0.93 ± 0.05	0.88	1.03	1.60	0.193
$^{168}Er/^{166}Er$	0.96 ± 0.04	0.90	1.02	0.99 ± 0.04	0.93	1.05	0.97 ± 0.06	0.92	1.08	1.00 ± 0.02	0.96	1.02	0.96 ± 0.06	0.90	1.05	1.23	0.312
$^{174}Yb/^{172}Yb$	0.97 ± 0.04^{b}	0.92	1.05	0.97 ± 0.02^{b}	0.92	0.99	0.98 ± 0.04^{b}	0.92	1.04	1.01 ± 0.03^{a}	0.98	1.06	1.00 ± 0.04^{ab}	0.96	1.06	3.23	0.022
$^{176}Lu/^{175}Lu$	1.10 ± 0.15	0.83	1.26	1.03 ± 0.12	0.84	1.27	1.09 ± 0.09	0.97	1.30	0.95 ± 0.09	0.82	1.07	1.05 ± 0.16	0.86	1.34	2.10	0.098

a–d Values with different superscripts differ significantly in terms of Pu'er tea in each year ($p < 0.05$).

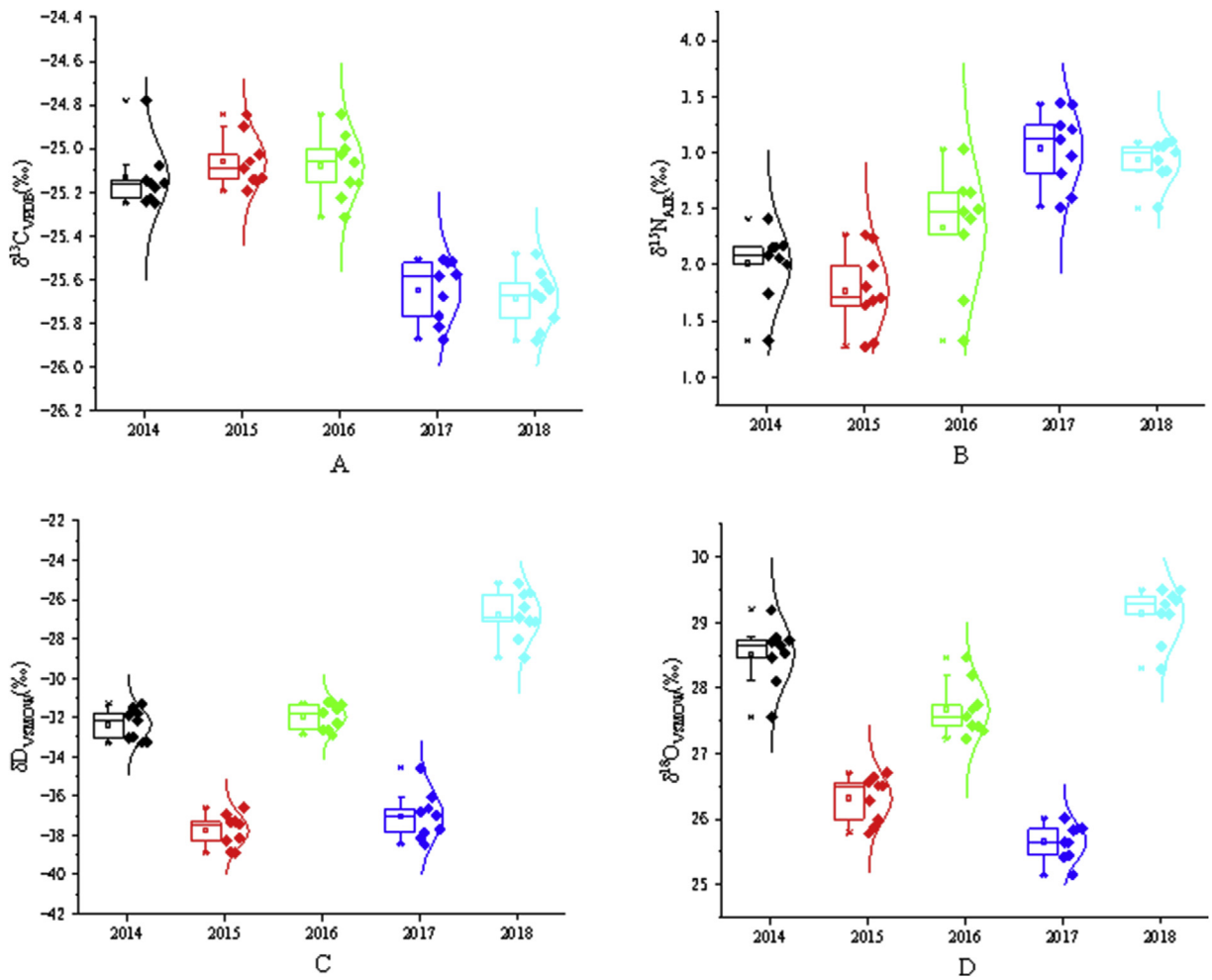

Fig. 1. Box/whisker charts of C N H O stable isotope ratios of Pu'er tea in five production years (from 2014 to 2018). The charts show the distribution of all data summarizing the variation in (A) $\delta^{13}C_{VPDB}$, (B) $\delta^{15}N_{AIR}$, (C) δD_{VSMOW}, and (D) $\delta^{18}O_{VSMOW}$ in the Pu'er tea samples in terms of the batches of different blend raw materials.

From 2014 to 2018 in Lincang, Yunnan, there has a great difference in annual climate, especially annual precipitation each year [40], which cause fractionation of this elements in a particular time frame. It probably could interpret the underlying mechanism of authentication of Pu'er teas using $\delta^{18}O$.

3.2. Variation in mineral element stable isotope ratios

The homogeneity and normal distribution of Pu'er tea were evaluated through one-way ANOVA with univariate variance. The mean and standard deviation of 39 different mineral element stable isotope ratios are summarized in Table 1. Some mineral element stable isotope ratios of Pu'er tea in five production years were significantly different ($p < 0.05$; Table 1). One-way ANOVA showed that 14 of the 39 mineral element stable isotope ratios in Pu'er tea ($^{138}Ba/^{137}Ba$, $^{114}Cd/^{111}Cd$, $^{72}Ge/^{70}Ge$, $^{74}Ge/^{70}Ge$, $^{53}Cr/^{52}Cr$, $^{98}Mo/^{96}Mo$, $^{96}Mo/^{95}Mo$, $^{98}Mo/^{95}Mo$, $^{208}Pb/^{207}Pb$, $^{48}Ti/^{47}Ti$, $^{154}Sm/^{152}Sm$, $^{158}Gd/^{156}Gd$, $^{160}Gd/^{156}Gd$, and $^{174}Yb/^{172}Yb$) significantly differed in the five production years. As indicated by Duncan's multiple comparison, Pu'er tea in 2014 had a characteristic mineral element stable isotope ratio fingerprint. In this study, $^{53}Cr/^{52}Cr$, $^{98}Mo/^{96}Mo$, $^{98}Mo/^{95}Mo$, and $^{154}Sm/^{152}Sm$ ratios were higher in Pu'er tea in 2014 than in other Pu'er tea. Pu'er tea in 2015 had a characteristic mineral element stable isotope ratio fingerprint of $^{48}Ti/^{47}Ti$. $^{114}Cd/^{111}Cd$ were higher in Pu'er tea in 2016 than in other Pu'er tea. Pu'er tea in 2017 had a characteristic mineral element stable isotope ratio profile of $^{138}Ba/^{137}Ba$ and $^{174}Yb/^{172}Yb$.And Pu'er tea in 2018 had a characteristic mineral element stable isotope ratio profile of $^{158}Gd/^{156}Gd$ and $^{160}Gd/^{156}Gd$.This result might be mainly due to the use of different chemical fertilizers from 2014 to 2018, which caused tea to absorb different minerals

from soil each year, and further studies should be conducted.

However, any difference could not be reliably distinguished with a single variable. Large differences were observed between the minimum multi-element stable isotope ratios and the maximum multi-element stable isotope ratios in the samples, which differed in the same year. Stoichiometric method that could accurately authenticate tea should be used to evaluate the clustering trend of the samples based on the 18 multi-element stable isotope ratios ($p < 0.05$) in five production years.

3.3. Exploratory statistical analysis

3.3.1. HCA

The levels of these 18 significant multi-element stable isotope ratios in Pu'er tea in five production years were subjected to HCA and PCA algorithms. HCA showed a cluster analysis tree of 18 multi-element stable isotope ratios ($p < 0.05$) in the samples (Fig. 2). HCA described three variable clusters. Group 1 contained $^{208}Pb/^{207}Pb$, $^{98}Mo/^{96}Mo$, $^{96}Mo/^{95}Mo$, $^{98}Mo/^{95}Mo$, $\delta^{13}C$, and $^{48}Ti/^{47}Ti$. The stable isotope ratios of Pb, Mo, and Ti could be in a cluster. Group 2 included δD, $\delta^{18}O$, $^{72}Ge/^{70}Ge$, $^{74}Ge/^{70}Ge$, and $^{53}Cr/^{52}Cr$. The stable isotope ratio of Cr and Ge could be in a cluster. δD and $\delta^{18}O$ that were influenced by irrigation water could also be in a cluster. Group 3 comprised $^{154}Sm/^{152}Sm$, $^{158}Gd/^{156}Gd$, $^{160}Gd/^{156}Gd$, $^{138}Ba/^{137}Ba$, $^{114}Cd/^{111}Cd$, $\delta^{15}N$, and $^{174}Yb/^{172}Yb$. The stable isotope ratios of rare earth elements (Yb, Gd, and Sm) could also be in a cluster. In this study, we found that the stable isotope ratios of some mineral elements (Pb, Mo, and Ti; Cr and Ge) were highly correlated to form a cluster. The correlation between the isotope ratios of these elements was attributed to the similarity of soil behavior in the genetic process from parent rock formation to diagenetic mineral weathering and leaching. However, this finding should be further verified. The stable isotope ratios that formed a cluster behaved similarly to Pu'er tea.

HCA revealed six sample clusters. Years 2014, 2015, 2017, and 2018 formed clear clusters, while 2016 is divided into two clusters (one individual and second as a part of 2017). HCA was conducted to accurately authenticate Pu'er tea in different production years by choosing 18 multi-element stable isotope ratios, which could not be specified.

3.3.2. PCA

PCA reduces the number of variables used in data description and is the most commonly used method for calculating components, such as linear potential variables. The unsupervised principal component

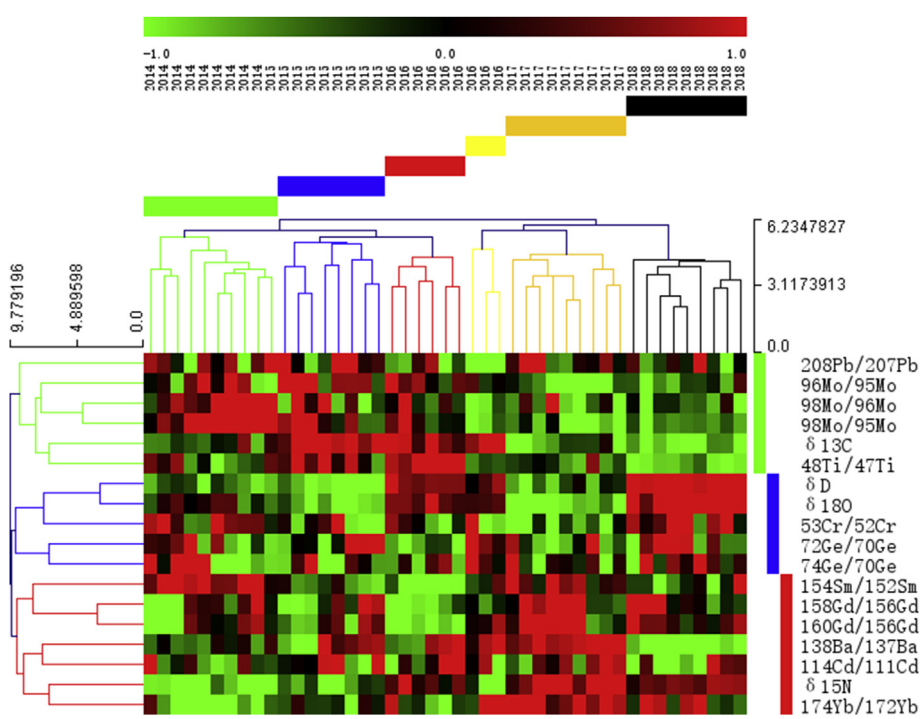

Fig. 2. Hierarchical clustering analysis (HCA) between variables and samples. Correlation coefficient is indicated by the intensity of colors as shown by the color scale. (2014, 2015, 2016, 2017, and 2018 indicate Pu'er tea in 2014, 2015 ', 2016', 2017', and 2018', respectively).

variance contribution rate and the load of 18 principal component variables used for the certification of Pu'er tea in the five studied years are shown in Fig. 3. In this study, the first three principal components (PCs) extracted in accordance with the Kaiser criterion represented PC1 (29.16%), PC2 (18.55%), and PC3 (13.38%; Fig. 3). The load-scattering diagrams of 18 variables showed that PC1 was strongly influenced by $\delta^{15}N$ and $^{174}Yb/^{172}Yb$. The key components of PC2 included $^{160}Gd/^{156}Gd$ and $^{158}Gd/^{156}Gd$. PC3 was basically contributed by $\delta^{18}O$ and δD (Fig. 3B, D).

PC1 and PC2 were the main components. The Pu'er tea could be preliminarily divided into five classes corresponding to 2014 to 2018 from the score plots for PC2 versus PC1 (Fig. 3A). Pu'er tea in 2014 showed negative scores in PC1 (the second and third quadrants), and this finding was easily differentiated from Pu'er tea in other years. A minimal overlap was found between Pu'er tea in 2015 and 2016, resulting in negative scores in PC2 (the third and fourth quadrants). Pu'er tea in 2017 with positive scores in PC1 and PC2 (the first quadrant) and Pu'er tea in 2018 with positive scores in PC1 (the first and fourth quadrants) could be easily differentiated from Pu'er tea in other years. The score plot for PC1 versus PC2 versus PC3 could show an improved differentiation among the scores corresponding to the different Pu'er tea in the five studied production years (Fig. 3C). However, different production years partially overlapped, and the PCA classification was not strong. In summary, the fractional scattering figure of Pu'er tea could be preliminarily divided into five classes based on the five studied production years under the orthogonal coordinate system of PC1, PC2, and PC3 on the basis of their 18 multi-element stable isotope ratio fingerprints.

The application of these two unsupervised methods of pattern recognition (HCA and PCA) revealed the natural grouping of the Pu'er tea in the

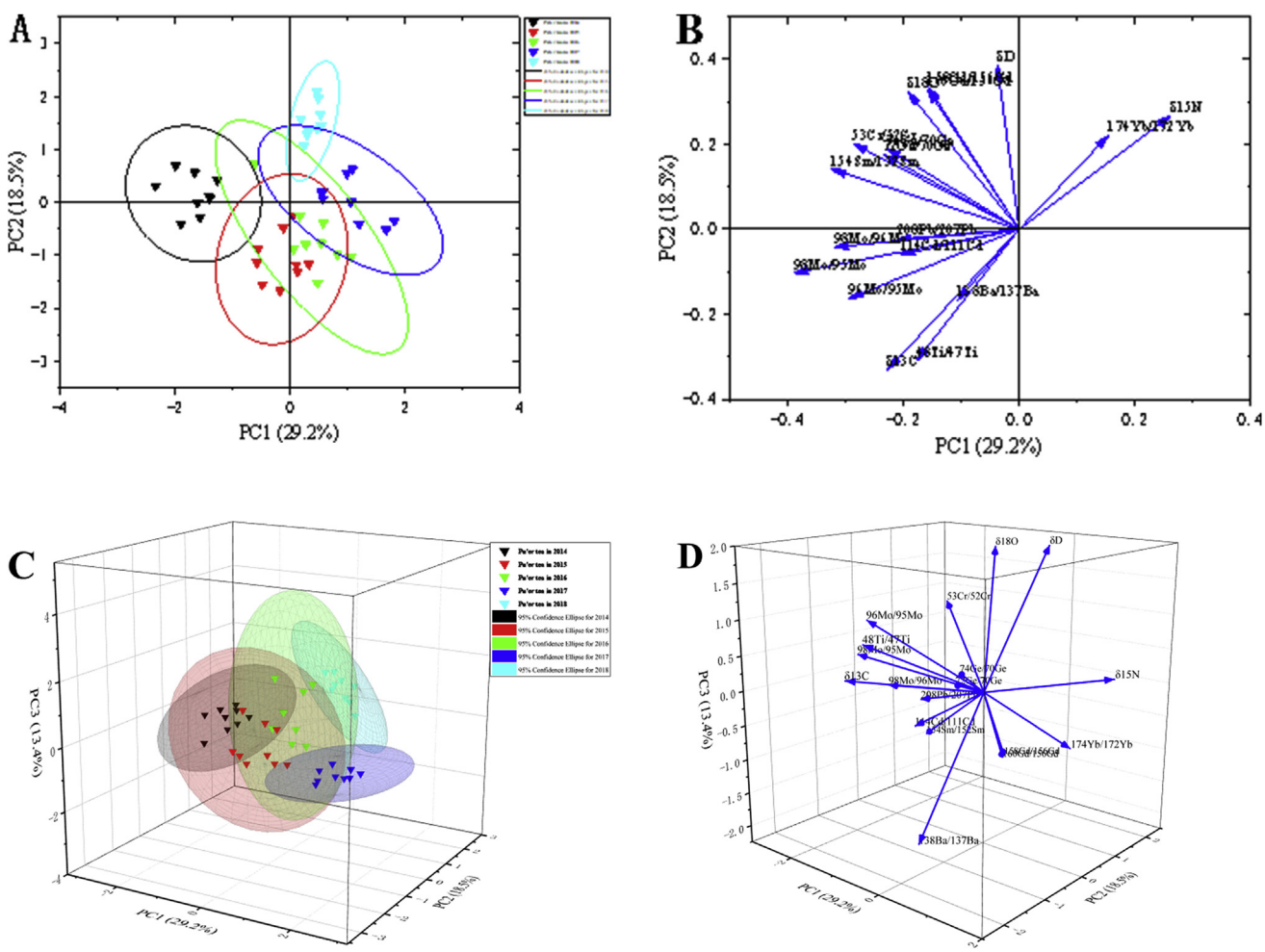

Fig. 3. PCA plots of multi-element stable isotope ratios showing the PC1, PC2, and PC3 effects to authenticate Pu'er tea in five production years (from 2014 to 2018). The ellipse on the score plots represents the 95% confidence region for Hotelling's T^2. Score plot of PC1 and PC2 (A), loading plot of PC1 and PC2 from PCA (B), Score plot of PC1, PC2 and PC3 (C), loading plot of PC1, PC2 and PC3 from PCA (D).

five studied production years in the original data matrix, indicating a tendency to group samples. Remarkably, HCA and PCA showed that Pu'er tea in the five studied production years slightly overlapped. Although HCA and PCA could provide a visual picture of how the samples were clustered, they could not present information about the quality of clustering and confidence in such clustering. Therefore, other supervised stoichiometric tools were further explored to authenticate Pu'er tea.

3.4. Classification and predictive modeling for sample authentication

PLS-DA, BP-ANN, and LDA models were established on the basis of the determination of 18 element stable isotope ratios in five Pu'er tea in different production years (from 2014 to 2018; $p < 0.05$) to use the multi-element stable isotope ratio for the authentication of these.

3.4.1. PLS-DA

PLS-DA is a projection method that maximizes the separation of observation groups by rotating PCA, which was an appropriate way to authenticate Pu'er tea in the five studied production years (Fig. 4). The PLS-DA score plot (Fig. 4A) was clear clustering, which revealed that the two highest-ranking R^2X accounted for 47.1% of the total variance. The first R^2X, accounting for 29.0% of this variance, separated the multi-element stable isotope ratio feature of the Pu'er tea in the five studied production years, which was 13.3% of this variance in the second R^2X. In PLS R^2X 1, the largest contributor was the highest stable isotope ratio of Mo in Pu'er tea in 2014 and indicated as eigenvectors of 0.418, 0.339, and 0.316 for $^{98}Mo/^{95}Mo$, $^{98}Mo/^{96}Mo$, and $^{96}Mo/^{95}Mo$, respectively. In R^2X 2, the largest contributors were $\delta^{13}C$, $^{138}Ba/^{137}Ba$, and $^{48}Ti/^{47}Ti$. The eigenvectors of $\delta^{13}C$, $^{138}Ba/^{137}Ba$, and $^{48}Ti/^{47}Ti$ were 0.340, 0.304, and 0.227, respectively (Fig. 4B). The variable importance in projection (VIP) value explains the contribution of variables in the projection; a VIP value of >1 is usually used to identify variables essential for modeling [41]. Six variables, namely, $^{138}Ba/^{137}Ba$ (VIP: 1.365), δD (VIP: 1.353), $\delta^{18}O$ (VIP:1.264), $\delta^{13}C$ (VIP: 1.200), $\delta^{15}N$ (VIP: 1.146), and $^{154}Sm/^{152}Sm$ (VIP: 1.133), were observed as

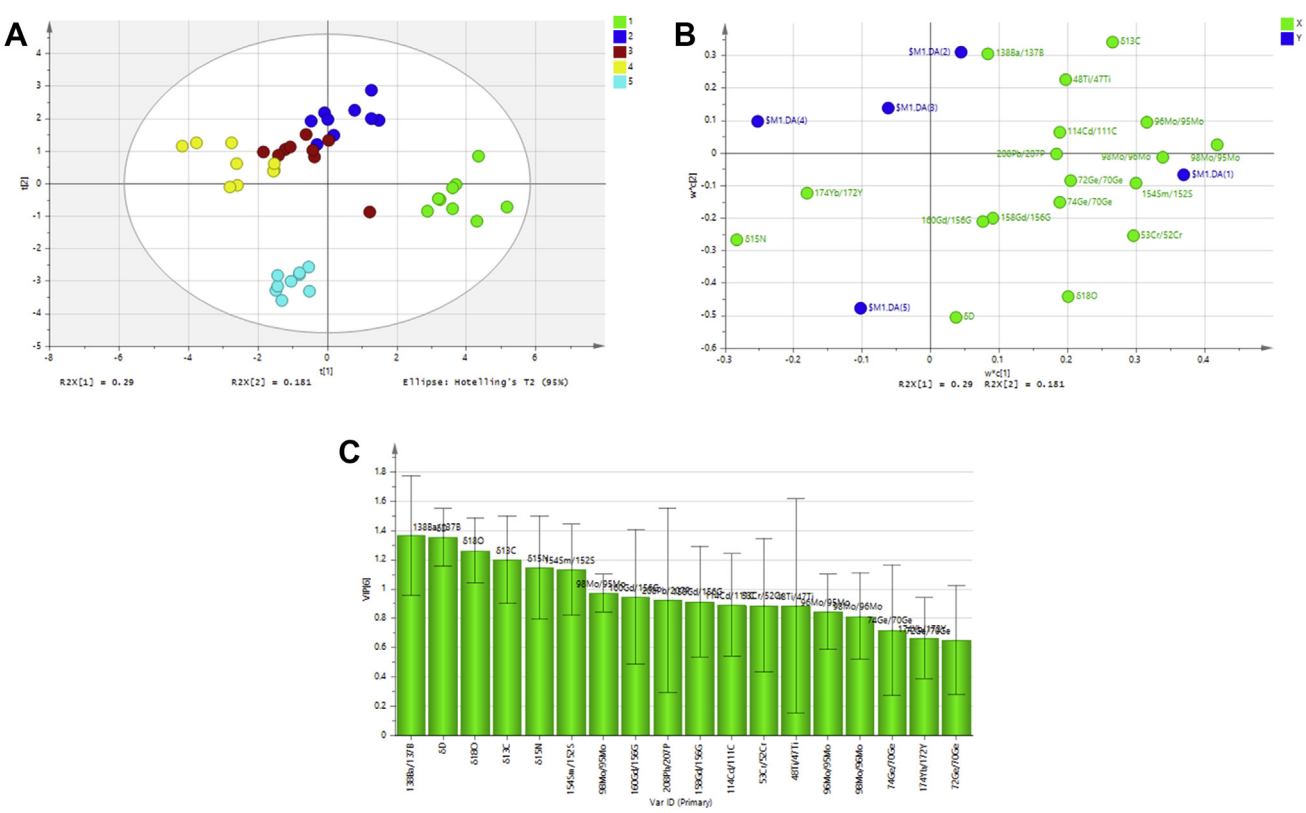

Fig. 4. Comparison of PLS-DA results derived from 18 multi-element stable isotope ratios of Pu'er tea in five production years (from 2014 to 2018). Score plot (A), loading plot from PLS-DA (B), and variable importance in projection (VIP) values obtained from the PLS-DA model (C). The ellipse on the score plots represents 95% confidence region for Hotelling's T^2. (1, 2, 3, 4, and 5 indicate Pu'er tea in 2014, 2015, 2016, 2017, and 2018, respectively).

significant multi-element stable isotope ratio features for the authentication of Pu'er tea (Fig. 4C).

Validation is critical to ensure the reliability of the developed PLS model because of the overfitting of PLS to the model, and data usually result in a split class score [42]. Although no threshold is set to compare criteria or determine importance, quality assessment statistics (Q^2) is usually the result of cross-validation [43]. In general, Q^2 greater than a 0.5 threshold indicates good predictability, whereas poor Q^2 corresponds to noisy data [44]. Our PLS-DA model displayed a good performance ($R^2X = 0.765$, $R^2Y = 0.843$, and $Q^2 = 0.666$) and explained 76.5% and 84.3% of the variations in X and Y, respectively, with a predictive Q^2 ability of 66.6%.

To our knowledge, the applicability of PLS-DA for tea authentication has never been reported. At present, multi-element stable isotope ratio analysis combined with PLS-DA provides a reliable Pu'er tea authentication in China. The PLS-DA score plot showed a cluster from Pu'er tea in different production years. However, a small overlap, which also existed in PCA, was observed between Pu'er tea in 2015 and 2016. This result could be attributed to their computational principles. PCA and PLS-DA can be applied to form components that capture most information in explanatory variables by maximizing the variance [35].

3.4.2. BP-ANN

A BP-ANN model was studied to further improve the authentication accuracy. In this study, a three-layer BP-ANN was established and applied to authenticate the Pu'er tea in different production years. The input and output layers had 18 and 5 neurons, respectively. The number of hidden layers was 1, and the number of neurons was 10. The recognition and prediction abilities of the model were evaluated.

In this study, 70% of the samples were randomly selected from Pu'er tea as a training set and cross-validation to evaluate the recognition ability. The remaining 30% of the samples were selected as the test set for the external verification test to evaluate the prediction ability. In the model training process, the five groups of Pu'er tea representing the corresponding production years could be successfully divided. In Table 2, the recognition ability of overall accuracy was 100.0% in all Pu'er tea. The remaining 30% of Pu'er tea were classified using the established model for external verification to further test the prediction ability of this model. Table 2 shows that 30% of the samples could be correctly predicted into the five groups. The overall prediction accuracy was 100.0%, indicating the good applicability of the proposed BP-ANN model.

In terms of the importance and standardization importance of variables in the BP-ANN (Table S1), the six most important variables as markers in the BP-ANN model were as follows: $\delta^{18}O$ (importance: 0.101, standardization importance: 100%), δD (importance: 0.088, standardization importance: 87.40%), $^{154}Sm/^{152}Sm$ (importance: 0.082, standardization importance: 81.70%), $\delta^{13}C$ (importance: 0.077,

Table 2. Model training and prediction results of the BP-ANN model.

	Pu'er tea in 2014	Pu'er tea in 2015	Pu'er tea in 2016	Pu'er tea in 2017	Pu'er tea in 2018	accuracy (%)
Model training						
Pu'er tea in 2014	5	0	0	0	0	100.0
Pu'er tea in 2015	0	6	0	0	0	100.0
Pu'er tea in 2016	0	0	7	0	0	100.0
Pu'er tea in 2017	0	0	0	7	0	100.0
Pu'er tea in 2018	0	0	0	0	3	100.0
Recognition ability (%)						100.0
Cross-validation						
Pu'er tea in 2014	5	0	0	0	0	100.0
Pu'er tea in 2015	0	6	0	0	0	100.0
Pu'er tea in 2016	0	0	7	0	0	100.0
Pu'er tea in 2017	0	0	0	7	0	100.0
Pu'er tea in 2018	0	0	0	0	3	100.0
Recognition ability (%)						100.0
Model test sets						
Pu'er tea in 2014	4	0.0	0.0	0.0	0	100.0
Pu'er tea in 2015	0.0	3	0.0	0	0	100.0
Pu'er tea in 2016	0.0	0.0	2	0.0	0	100.0
Pu'er tea in 2017	0.0	0.0	0	2	0	100.0
Pu'er tea in 2018	0	0	0	0	6	100.0
prediction ability (%)						100.0

standardization importance: 76.70%), $^{138}Ba/^{137}Ba$ (importance: 0.073, standardization importance: 72.30%), and $^{48}Ti/^{47}Ti$ (importance: 0.068, standardization importance: 67.30%). The performance of the BP-ANN model was more accurate than that of the PLS-DA method.

3.4.3. LDA

The LDA model was also used to further improve the authentication accuracy. The recognition and prediction abilities of the LDA model were also evaluated. The Pu'er tea were divided into training sets, cross-validation (70% of samples) and test sets (30% of samples) for external validation. The recognition capability of the model was examined with the training set, whereas the prediction ability was verified through cross-validation and external validation. The results showed that two statistically significant discriminant Fisher functions were formed: Wilks' lambda = 0.000, X^2 = 207.895, df = 20, $p < 0.001$ for the first Fisher function, and Wilks' lambda = 0.015, X^2 = 108.972, df = 12, $p < 0.001$ for the second Fisher function. A significant Wilks' lambda indicated that the discriminant function was the basis for differentiating populations. The testing of the uniformity of variability (Box M index = 111.636, F = 1.039, p = 0.396) was not significant at 95% confidence level, suggesting that the variability of the samples in each production year was consistent. The first discriminant Fisher function accounted for 77.4% of the total variance, and the second discriminant Fisher function accounted for 14.2%. Both accounted for 91.6% of the total variance, showing a high level. After forward stepwise variable selection based on Wilk's lambda criterion, δD, $\delta^{13}C$, $\delta^{15}N$, $^{98}Mo/^{95}Mo$, and $^{154}Sm/^{152}Sm$ were five variables that factored into the simplified model.

Discriminant analysis showed that the Pu'er tea in different production years were well authenticated (Fig. 5). The first discriminant function showed an evident authentication function for Pu'er tea in 2015 and 2018 compared with that in the other years. The second discriminant function had an evident identification function for Pu'er tea in 2014 and 2017 compared with that in the other years. Recognition ability was expressed as the percentage of Pu'er tea in different production years correctly classified during model training, with an overall accuracy of 100.0%, indicating an excellent result. The prediction ability was expressed as the percentage of Pu'er tea in different production years correctly classified using a typical cross-validation procedure and an external validation procedure. The overall prediction accuracy was 100.0% for cross-validation and external validation methods. This result suggested a satisfactory value, especially for this method (Table S2). The multi-element stable isotope ratios

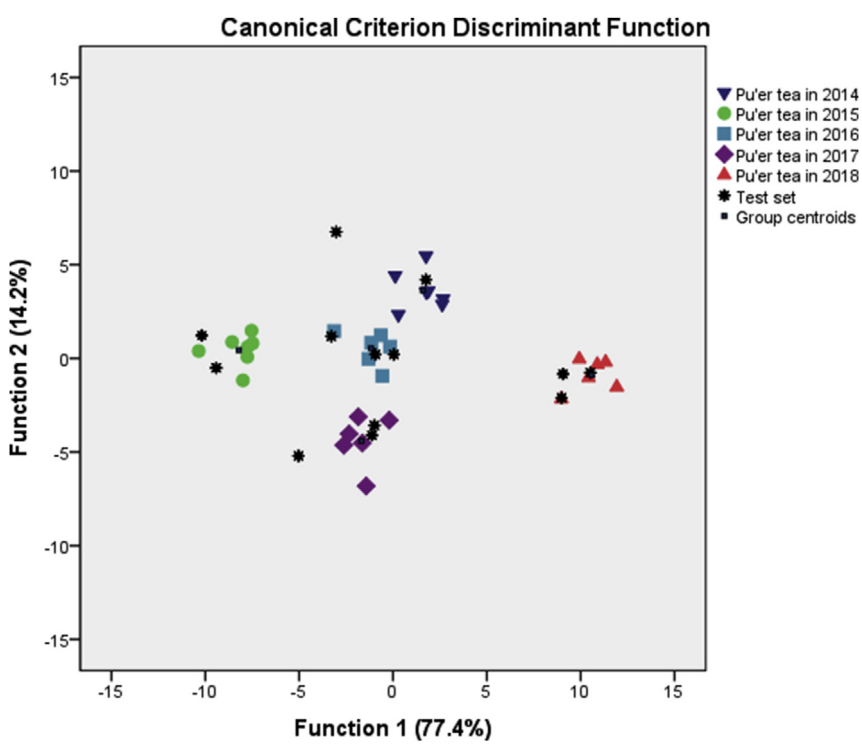

Fig. 5. Authentication of Pu'er tea in five production years (from 2014 to 2018) based on the 18 multi-elemental stable isotope ratios ($p < 0.05$).

(independent variables) constituting the first and second discriminant functions are shown in Table S3. δD strongly influenced the first discriminant function. This finding showed that Pu'er tea in 2015 was the most positive, whereas the four other stable element isotope ratios mainly contributed to the second discriminant functions.

The performance of separation between the groups in BP-ANN and LDA was better than that of PLS-DA possibly because of different training algorithms. BP-ANN training involves multiple perception levels, whereas the goal of LDA is to project high-dimensional data into a low-dimensional space and obtain the maximum class discrimination through the ratio of the maximum interclass and intraclass distances [36,37]. Among the variables selected through different methods, the three models shared δD, $\delta^{13}C$, and $^{154}Sm/^{152}Sm$ as markers of Pu'er tea in different production years.

4. Conclusions

The fingerprints of Pu'er tea in five production years (from 2014 to 2018) consisted of 43 multi-elemental stable isotope ratios and were obtained through EA-IRMS and ICP-MS. These techniques are reliable tools for generating chemical information-rich multi-elemental stable isotope ratio fingerprints. This study confirmed that 18 statistically significant multi-elemental stable isotope ratio signatures could be applied as fingerprints to authenticate Pu'er tea. This study also demonstrated significant differences in some of the multi-elemental stable isotope ratios and Pu'er tea in different production years by projecting the multi-elemental stable isotope ratio data on the computing platform of two unsupervised and three supervised learning techniques. The clustering ability of the two unsupervised learning methods were worse than that of the three supervised learning methods. The supervised models proposed using the LDA, PLS-DA, and BP-ANN algorithms showed that the authentication performance of BP-ANN and LDA was better than that of PLS-DA, with a recognition ability of 100% and a prediction ability of 100%. δD, $\delta^{13}C$, and $^{154}Sm/^{152}Sm$ were the markers for enabling the accurate authentication of Pu'er tea in different production years.

In conclusion, we developed a feasible method for multi-elemental stable isotope ratio analysis and improved the process of identifying the authenticity of tea by using a stoichiometric model. Our study could enhance the authentication procedures for existing tea and facilitate the detection of fake brand labels. The established prediction model had the advantages of high accuracy, strong robustness, human factor independence, and so on. As such, it had a certain application prospect in food classification and group distribution, especially in food source traceability and adulteration research. This work presented the great potential of multi-elemental stable isotope ratio fingerprinting for evaluating the authenticity of foods, such as tea. However, our results must be interpreted cautiously, as a limited number of Pu'er tea samples were tested. Future studies should evaluate a larger number of Pu'er tea samples from different years to establish global isotope markers for reliable authentication on a wider scale.

Declaration of Competing Interest

All authors declare that they have no conflict of interest.

Acknowledgements

This paper was supported by Southwest University and Chongqing University of Education in 2019; Chongqing modern mountain characteristics efficient agricultural tea industry technical system 2019-6,2018-6; Project funded by Chongqing university innovation team construction plan (CXTDX201601040). The authors thank the reviewers for their perceptive and helpful comments.

Appendix A. Supplementary data

Supplementary data to this article can be found online at https://doi.org/10.38212/2224-6614.1059.

References

[1] Khan N, Mukhtar H. Tea polyphenols for health promotion. Life Sci 2007;81:519–33.
[2] Zhang JY, Guicen M, Chen LY, Liu T, Liu X, Lu CY. Profiling elements in Puerh tea from Yunnan province, China. Food Addit Contam B 2017;10(3):155–64.
[3] Lv SD, Wu YS, Li CW, Xu YQ, Liu L, Meng QX. Comparative Analysis of Pu-erh and Fuzhuan teas by fully automatic headspace solid-phase microextraction coupled with gas chromatography-mass spectrometry and chemometric methods. J Agric Food Chem 2014;62:1810–8.
[4] Lv HP, Zhang YJ, Lin Z, Liang YR. Processing and chemical constituents of Pu-erh tea: a review. Food Res Int 2013;53:608–18.
[5] Hou Y, Shao WF, Xiao R, Xu KL, Ma ZZ, Johnstone BH, et al. Pu-erh tea aqueous extracts lower atherosclerotic risk factors in a rat hyperlipidemia model. Exp Gerontol 2009;44:434–9.
[6] Lv HP, Zhu Y, Tan JF, Guo L, Dai WD, Lin Z. Bioactive compounds from Pu-erh tea with therapy for hyperlipidaemia. J Funct Foods 2015;19:194–203.
[7] Cap YN, Liu TX. Analysis of aroma composition in Pu-erh raw and ripe teas with different storage time. Food Ind 2011:64–7.

[8] Li F, Lu QH, Li M, Yang XM, Xiong CY, Yang B. Comparison and risk assessment for trace heavy metals in raw Pu-erh tea with different storage years. Biol Trace Elem Res 2020;195(2): 696–706.

[9] Xue DW, Yang CL, Kong HF, Bao JH. An electronic nose-based method for determination of the storage time of huangshan maofeng tea. Mod Food Sci Technol 2016;3: 64–7.

[10] Yang XM, Liu YL, Mu LH. Discriminant research for identifying aromas of non-fermented Pu-erh tea from different storage years using an electronic nose. J Food Process Preserv 2018;42(10):e13721.

[11] Xie DC, Dai WD, Lu ML, Tan JF, Zhang Y, Chen M, et al. Nontargeted metabolomics predicts the storage duration of white teas with 8-C N-ethyl-2-pyrrolidinone-substituted flavan-3-ols as marker compounds. Food Res Int 2019;125. UNSP 108635.

[12] Lv SD, Wu YS, Wei JF, Lian M, Wang C, Gao XM, et al. Application of gas chromatography-mass spectrometry and chemometrics methods for assessing volatile profiles of Pu-erh tea with different processing methods and ageing years. RSC Adv 2015;5(107):87806–17.

[13] Ning JM, Zhnag ZZ, Wang SP, Wan XC, Zeng XS. Identification of Pu'er teas with different storage years by FTIR spectroscopy. Spectrosc Spectral Anal (Beijing, China) 2011; 31(9):2390–3.

[14] Xu SS, Wang JJ, Wei YM, Deng WW, Wan XC, Bao GH, et al. Metabolomics based on UHPLC-Orbitrap-MS and global natural product social molecular networking reveals effects of time scale and environment of storage on the metabolites and taste quality of raw Pu-erh tea. J Agric Food Chem 2019; 67(43):12084–93.

[15] Mirasoli M, Gotti R, Di Fusco M, Leoni A, Colliva C, Roda A. Electronic nose and chiral-capillary electrophoresis in evaluation of the quality changes in commercial green tea leaves during a long-term storage. Talanta 2014;129:32–8.

[16] Han DK, Bae JY, Hyon SH. Biochemical and histological evaluations of articular cartilages preserved in cold storage solution containing green tea catechin:EGCG. J Tissue Eng Regen Med 2009;6:380–7.

[17] Kidist T, Adugna D, Weyessa G. Effect of drying temperature and duration on biochemical composition and quality of black tea (Camellia sinensis L.) O Kuntze at Wush, south western Ethiopia. Asian J Plant Sci 2013;12:235–40.

[18] Ni K, Wang J, Zhang QF, Yi XY, Ma LF, Shi YZ, et al. Multi-element composition and isotopic signatures for the geographical origin discrimination of green tea in China: a case study of Xihu Longjing. J Food Compos Anal 2018;67: 104–9.

[19] Liu Z, Yuan YW, Zhang YZ, Shi YZ, Hu GX, Zhu JH, et al. Geographical traceability of Chinese green tea using stable isotope and multi-element chemometrics. Rapid Commun Mass Spectrom 2019;33:778–88.

[20] Lou YX, Fu XS, Yu XP. Stable isotope ratio and elemental profile combined with support vector machine for provenance discrimination of oolong tea (Wuyi-Rock tea). J Anal Methods Chem 2017:5454231.

[21] Cengiz MF, Turan O, Ozdemir D, Albayrak Y, Perincek F, Kocabas H. Geographical origin of imported and domestic teas (Camellia sinensis) from Turkey as determined by stable isotope signatures. Int J Food Prop 2017;20(12):3234–43.

[22] Chang CT, You CF, Aggarwal SK, Chung CH, Chao HC, Liu HC. Boron and strontium isotope ratios and major/trace elements concentrations in tea leaves at four major tea growing gardens in Taiwan. Environ Geochem Health 2016; 38:737–48.

[23] Rajapaksha D, Waduge V, Padilla-Alvarez R, Kalpage M, Rathnayake RMNP, Migliori A, et al. XRF to support food traceability studies:Classification of Sri Lankan tea based on their region of origin. X Ray Spectrom 2017;46:220–4.

[24] Zhang L, Pan JR, Zhu C. Determination of the geographical origin of Chinese teas based on stable carbon and nitrogen isotope ratios. J Zhejiang Univ Sci B 2012;13(10):824–30.

[25] Wu C, Yamada K, Sumikawa O, Matsunaga A, Gilbert A, Yoshida N. Development of a methodology using gas chromatography-combustion-isotope ratio mass spectrometry for the determination of the carbon isotope ratio of caffeine extracted from tea leaves(Camellia sinensis). Rapid Commun Mass Spectrom 2012;26:978–82.

[26] Lagad RA, Alamelu D, Laskar AH, Rai VK, Singh SK, Aggarwal SK. Isotope signature study of the tea samples produced at four different regions in India. Anal Methods 2013;5:1604.

[27] Farquhar GD, Ehleringer JR, Hubick KT. Carbon isotope discrimination and photosynthesis. Annu Rev Plant Physiol Plant Mol Biol 1989;40:503–37.

[28] Brugnoli E, Farquhar GD. Phtosynthesis: physiology and metabolism. Dordrecht: Kluwer Academic Publishers; 2000.

[29] Bateman AS, Kelly SD. Fertilizer nitrogen isotope signatures. Isot Environ Health Stud 2007;43:237–47.

[30] Gremaud G, Hilkert A. Isotopic-spectroscopic technique: stable isotope ratio mass spectrometry (IRMS). In: Sun DW, editor. Modern techniques for food authentication. Burlington, MA, USA: Academic Press; 2008. p. 269–320.

[31] Kelly S, Heaton K, Hoogewerff J. Tracing the geographical origin of food: the application of multi-element and multi-isotope analysis. Trends Food Sci Technol 2005;16:555–67.

[32] Choi WJ, Ro HM, Lee SM. Natural ^{15}N abundances of inorganic nitrogen in soil treated with fertilizer and compost under changing soil moisture regimes. Soil Biol Biochem 2003;35:1289–98.

[33] Lagad RA, Singh SK, Rai VK. Rare earth elements and $^{87}Sr/^{86}Sr$ isotopic characterization of Indian Basmati rice as potential tool for its geographical authenticity. Food Chem 2017;217:254–65.

[34] Stanimirova I, Daszykowski M, Walczak B. Dealing with missing values and outliers in principal component analysis. Talanta 2007;72(1):172–8.

[35] Wold S, Ruhe A, Wold H, Dunn W. Collinearity problem in linear regression. The partial least squares (PLS) approach to generalized inverses. J Sci Stat Computations 1984;5(3): 735–43.

[36] Zupan J, Gasteiger J. Neural networks: a new method for solving chemical problems or just a passing phase. Anal Chim Acta 1991;248(1):1–30.

[37] Moncayo S, Manzoor S, Caceres JO. Chemometrics and intelligent laboratory systems evaluation of supervised chemometric methods for sample classi fication by laser induced breakdown spectroscopy. Chemometr Intell Lab Syst 2015; 146:354–64.

[38] Hoefs J. Stable isotope geochemistry. Berlin: Springer; 1997.

[39] Bateman AS, Kelly SD, Woolfe M. Nitrogen isotope composition of organically and conventionally grown crops. J Agric Food Chem 2007;55:2664–70.

[40] China Meteorological Administration. Near-surface meteorological observation data obtained by various observationmeans and derived data derived from comprehensive analysis. Retrieved December 01 2019, available from, http://data.cma.cn/data/index/f0fb4b55508804ca.html. 2019.

[41] Jumtee K, Bamba T, Fukusaki E. Fast GC-FID based metabolic fingerprinting of Japanese green tea leaf for its quality ranking prediction. J Separ Sci 2009;32:2296–304.

[42] Westerhuis JA, Hoefsloot HCJ, Smit S, Vis DJ, Smilde AK, Velzen EJJ, et al. Assessment of PLS-DA cross validation. Metabolomics 2008;4:81–9.

[43] Worley B, Powers R. Multivariate analysis in metabolomics. Curr Metabolomics 2013;1:92–107.

[44] Eriksson I, Johansson E, Kettaneh-Wold N, Wold S. Multi- and megavariate data analysis principles and applications. Sweden: Umetrics AB: Umeå; 2001.